VELOCITY PROFILES OF DEVELOPING AND DEVELOPED OPEN CHANNEL FLOW

By M. Salih Kırkgöz[1] and Mehmet Ardıçlıoğlu[2]

ABSTRACT: Using a Laser-Doppler anemometer, mean velocities are measured in developing and fully developed turbulent subcritical smooth open channel flows. Experiments are conducted in a rectangular laboratory channel for 12 different test conditions with Reynolds number ranging from 28,026 to 136,842. From the experiments it is found that the boundary layer along the centerline of the channel develops up to the free surface for a flow aspect ratio $b/h \geq 3$. Shear velocities are calculated using the measured velocity profiles in the viscous sublayer of the boundary flow. The experiments show that shear velocity varies in an oscillatory manner across the flow section around $b/h = 3$. In the turbulent inner regions of developing and fully developed boundary flows, the measured velocity profiles agree well with the logarithmic "law of the wall" distribution when the coefficients in the expression are 2.44 and 5.5, respectively. The "wake" effect becomes important in the velocity profiles of the fully developed boundary layers. A reasonable agreement between the modified velocity-defect law and the experimental profile in the inner and outer regions is obtained with a profile parameter of 0.1 in the Coles's "law of the wake."

INTRODUCTION

The two-dimensional mean velocity distribution of open channel flow is important in the analysis of wall friction and sediment transport phenomenon. With the employment of sophisticated measuring devices such as hot-film anemometry (Bayazit 1976; Gaddini and Morganti 1982; Zippe and Graf 1983) and Laser-Doppler anemometry (Nezu and Rodi 1986; Kırkgöz 1989; Maclean 1991; Tominaga and Nezu 1992) the experimental investigations of the velocity profiles, particularly near the solid boundaries, increasingly have produced practically useful information for open channel problems. Especially, the employment of the Laser-Doppler anemometer allows the velocities to be measured very close to the wall without disturbing the flow.

At the entrance to a channel a high-velocity gradient is developed in the vicinity of channel bed, which is associated with the frictional stresses generated between the fluid particles and the solid walls. The layer of fluid adjacent to a solid boundary where viscous effects are evident is called the "boundary layer" (Fig. 1). The boundary layer, which may be laminar at the upstream end, steadily thickens up to a certain point in the channel length L in which the flow is called "developing flow"; beyond this location the flow is called "fully developed flow." For smooth boundaries the viscous effects persist in a very thin film called "viscous sublayer" in which the greater part of the velocity change occurs. In fully developed turbulent flow, with regard to the velocity controlling parameters, the boundary layer is composed of two distinct regions: the inner region and the outer region. The inner region consists of two parts: the viscous sublayer and the fully turbulent inner region. More details on the topic may be found in Cebeci and Smith (1974). In Fig. 1 δ represents the boundary layer thickness and h represents the flow depth.

Experimental investigations on velocity measurements for fully developed open channel flow are available. However, the experimental data for the developing zone are not satisfactory.

[1]Prof. of Hydr., Civ. Engrg. Dept., Çukurova Univ., 01330 Adana, Turkey.

[2]Asst. Prof. of Hydr., Civ. Engrg. Dept., Erciyes Univ., 38039 Kayseri, Turkey.

In this study, mean velocities are measured using a Laser-Doppler anemometer in the developing and the fully developed turbulent subcritical smooth open channel flows. The "law of the wall" and the "velocity-defect" distributions of the mean velocity profiles are presented. The shear velocity of each profile is determined using the measured velocities in the viscous sublayer.

VELOCITY DISTRIBUTION FORMULAS

In the past, various semiempirical models have been used to represent the velocity profiles of fully developed turbulent open channel flow. Some of the widely used expressions for this purpose are given in the following.

In the inner region of the turbulent boundary layer on a smooth wall, the flow velocities are controlled by the wall shear stress τ_0, the distance from the wall z and the kinematic viscosity ν of the fluid. The velocity distribution in the viscous sublayer generally is admitted linear. In the fully turbulent layer of the inner region, the logarithmic velocity distribution of von Kármán (1930), Prandtl (1932), known as the law of the wall, is the universally accepted formula

$$\frac{u}{u_*} = A \ln \frac{u_* z}{\nu} + B \tag{1}$$

where $A = 1/\chi$, χ = von Kármán constant; $B = a$ constant, $u_*(=\sqrt{\tau_0/\rho})$ = shear velocity; and ρ = density. Although the value of B depends on the nature of the wall surface, the value of A does not (Schlichting 1968). Nikuradse (1932), in his experiments, found that $A = 2.5$ and $B = 5.5$ for hydraulically
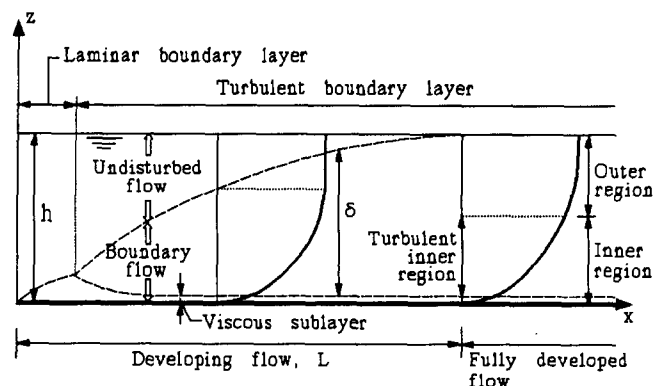

FIG. 1. Velocity Profiles in Developing and Fully Developed Open Channel Flow

"smooth" pipe flow and Keulegan (1938) assumed that the same values can be used for smooth open channel flow as well. In a recent study, Kirkgöz (1989) confirmed these results. However, different values for A and B have been obtained by various investigators. The value of A has a range of variation between 2.43 (Nezu and Rodi 1986) and 2.5 (Steffler et al. 1985) and B between 4.9 (Klebanoff 1954) and 7 (Townsend 1956).

Coles (1956) introduced the wake hypothesis in (1) to extend the law of the wall to the outer region of boundary layer. He gave the expression in the form

$$\frac{u}{u_*} = \frac{1}{\chi} \ln \frac{u_* z}{\nu} + B + \frac{\Pi}{\chi} w \left(\frac{z}{\delta} \right) \qquad (2)$$

where Π = a "profile" parameter; and $w(z/\delta)$ = an empirical "wake" function or, as he called, the "law of the wake" given by $2 \sin^2(\pi z/2\delta)$. Coles (1956) showed that for $\chi = 0.4$, $B = 5.1$, and $\Pi = 0.55$ there was reasonable agreement between the experiments and (2).

In the outer region of boundary layer where the flow velocities mainly are controlled by turbulent shear, the velocity-defect law is suitable for both smooth and "rough" walls (Prandtl 1925). That is

$$\frac{u_m - u}{u_*} = -\frac{1}{\chi} \ln \frac{z}{\delta} \qquad (3)$$

where u_m = maximum velocity in the distribution. Some correction terms were added to (3) for a better fit with experimental data; for instance, a correction value of 2.5 was added by Clauser (1956).

The velocity-defect form of the wake hypothesis due to Coles can be obtained from (2) as

$$\frac{u_m - u}{u_*} = -\frac{1}{\chi} \ln \frac{z}{\delta} + \frac{\Pi}{\chi} 2 \cos^2 \left(\frac{\pi z}{2\delta} \right) \qquad (4)$$

Different values for the profile parameter Π have been suggested such as 0.2 by Nezu and Rodi (1986) for $R \geq 10^5$ and 0.1 by Kırkgöz (1989). These are considerably smaller than 0.55 given by Coles.

EXPERIMENTS

Experiments were carried out at the Hydraulics Laboratory of the Çukurova University, Adana, Turkey. The glass-walled laboratory channel was 9.5 m long, 0.3 m wide, and 0.4 m deep. The channel bed was covered with a glass layer, which was thought suitable for a smooth-wall experiment. Flow rates were measured using a KROHNE UFM600 type ultrasonic flowmeter and flow velocities were measured by a DISA 55L67 type Laser-Doppler anemometer.

Flow velocities were measured at 11 midverticals ($x = 1.1$, 1.7, 2.5, 3.0, 3.5, 4.0, 4.5, 5.0, 5.5, 6.0, and 6.5 m) along the flow developing zone and at seven verticals ($y = 0.02$, 0.04, 0.06, 0.08, 0.1, 0.12, and 0.14 m) across the half-width of the
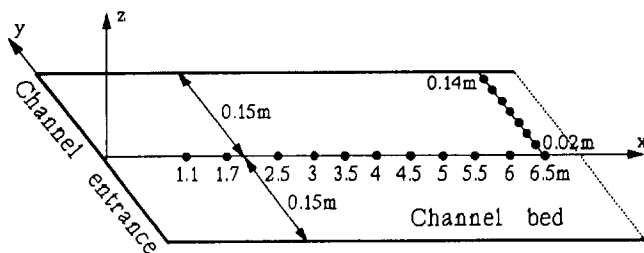

FIG. 2. Positions of Verticals for Velocity Measurements

TABLE 1. Details of Experimental Conditions

Test number (1)	Q (L/s) (2)	h (mm) (3)	b/h (4)	L (m) (5)	F (6)	R (7)
1	3.2	50	6.00	3.5	0.30	28,026
2	3.2	25	12.00	1.7	0.85	32,062
3	6.0	75	4.00	4.5	0.31	46,842
4	6.0	60	5.00	4.0	0.43	50,125
5	6.0	45	6.67	3.0	0.67	53,903
6	10.0	100	3.00	5.0	0.34	70,105
7	10.0	60	5.00	4.0	0.72	83,693
8	14.5	200	1.50	6.5	0.23	97,728
9	14.5	80	3.75	5.0	0.68	110,627
10	19.5	150	2.00	6.5	0.36	113,947
11	19.5	120	2.50	6.0	0.50	126,847
12	19.5	100	3.00	5.5	0.66	136,842

flow section at $x = 6.5$ m. Fig. 2 shows the positions of the verticals for the velocity measurements. The $x = 0$ refers to the entrance of the channel and therefore represents the initial position of the flow developing zone. The end of the flow development was determined by comparing the velocity profiles measured along the channel. It was found that the length of the flow developing zone varies between 1.7 and 6.5 m depending on the flow conditions. Consequently, the section at $x = 6.5$ m was assumed to represent the fully developed flow section for all tests.

Experiments were conducted for 12 different subcritical uniform flow conditions. The details of the test conditions are given in Table 1 in which Q is the discharge, b/h is the flow aspect ratio, L is the length of the flow developing zone, F $(=V/\sqrt{gh})$ is the Froude number, V is the average velocity of flow, R $(=4VR/\nu)$ is the Reynolds number, and R is the hydraulic radius. The tests in Table 1 are numbered in increasing order of Reynolds number.

RESULTS AND ANALYSIS

Length of Flow Developing Zone

In Fig. 3, the dimensionless length of the flow developing zone L/h is plotted against the ratio R/F, based on the flow parameters given in Table 1. From the experimental data in Fig. 3, the correlation between the dimensionless length of the developing zone with Reynolds number and Froude number may be approximated by the following simple expression:

$$\frac{L}{h} = 76 - 0.0001 \frac{R}{F} \qquad (5)$$

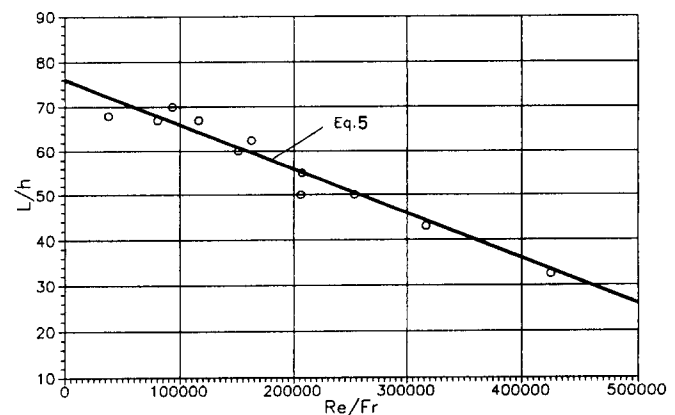Eq. (5) is suggested for predicting the length of the flow de-

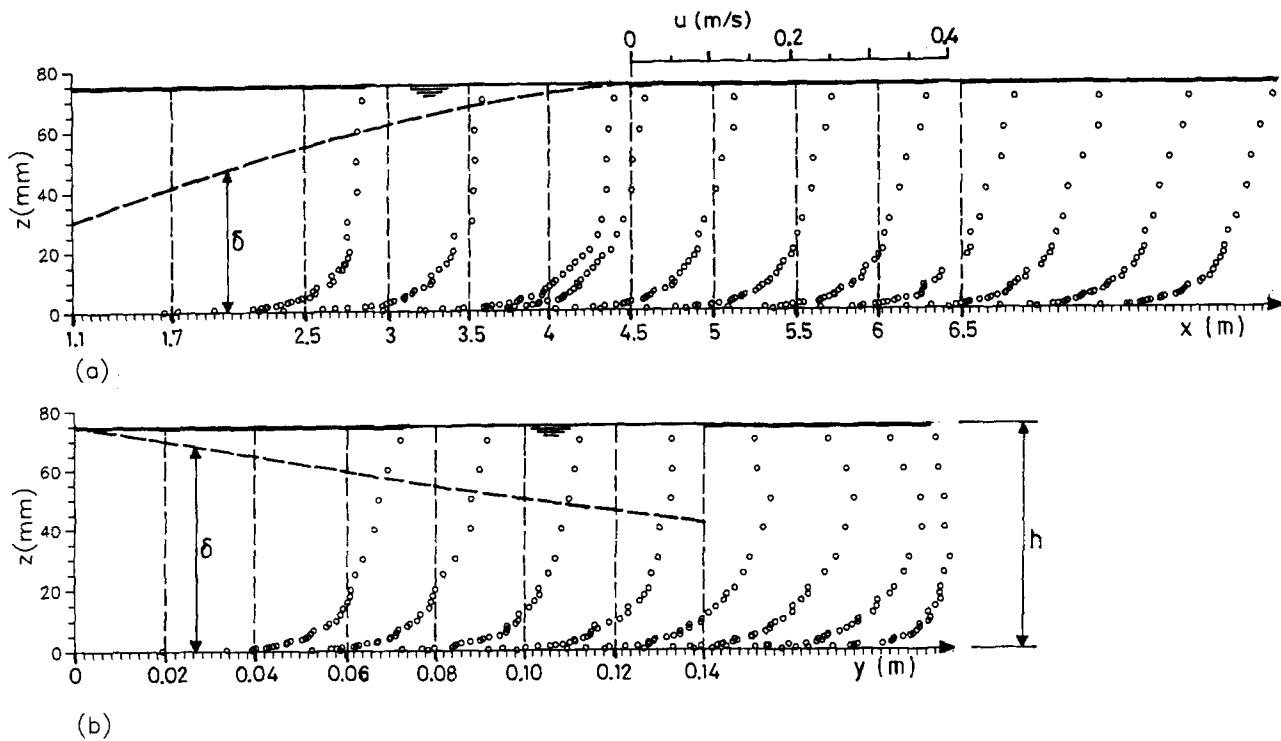**FIG. 3. Variation of Dimensionless Length of Flow Developing Zone with R/F**

FIG. 4. Measured Velocity Profiles for Test 3: (a) along Developing Flow at $y = 0$; (b) across Flow Section at $x = 6.5$ m
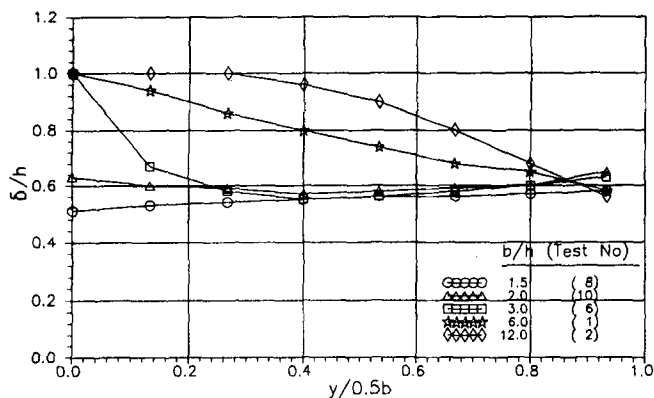

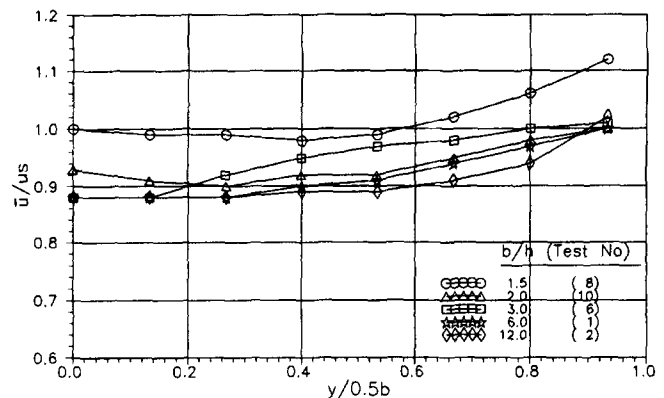FIG. 5. Variation of δ/h across Fully Developed Flow Section

FIG. 6. Variation of $\bar{u}/u_s$ across Fully Developed Flow Section

veloping zone of open channel flow within the present experimental conditions.

Features of Velocity Profiles

Fig. 4 shows the measured velocity profiles for test 3. All measured velocity profiles for 12 tests are given in Ardıçlıoğlu (1994). Fig. 4(a) gives the velocity profiles along the centerline of the developing flow. By examining the velocity profiles in Fig. 4(a) it may be seen that the vertical distribution of the velocities remains almost unchanged and consequently the flow can be assumed fully developed when $x \geq 4.5$ m, for test 3. That is, the length of the boundary layer development is $L = 4.5$ m for this particular case. The measured velocity profiles of 12 tests show that the length of the boundary layer development varies between $50h$ and $70h$. Fig. 4(a) shows that the thickness of the boundary layer δ gradually increases and at the end of the developing zone δ becomes equal to the flow depth h. Fig. 4(b) shows the velocity profiles across the flow section at $x = 6.5$ m. It is observed that δ decreases steadily toward the sidewall. The creation of the dip in the velocity profiles across the channel is attributed to the secondary currents generated by the combined action of the bed and sidewall boundary layers in the corner area.

Fig. 5 gives the variation of boundary layer thickness across the channel width for five tests of different aspect ratios. From these and other tests it may be concluded that the boundary layer thickness at the midvertical of a fully developed open channel flow becomes equal to the water depth when $b/h \geq 3$. For $b/h = 1.5$ the ratio δ/h takes a value of 0.51 at $y = 0$ and then slightly increases toward the sidewall. For $b/h = 2$, δ/h equals 0.63 at the centerline and following a slight decrease, subsequently, it increases near the sidewall. For $b/h = 3$, δ/h rapidly decreases first and then follows a similar trend to the preceding two cases. The variation of δ/h for $b/h = 12$ in Fig. 5 indicates that as the aspect ratio increases, the middle portion of the channel where $\delta = h$ tends to widen.

Fig. 6 gives the variation of the ratio of vertical mean velocity for unit width and the surface velocity $\bar{u}/u_s$ across the fully developed flow section. For $y/0.5b \leq 0.6$, $\bar{u}/u_s$ varies between 0.88 and 1.00 for aspect ratios between 1.5 and 12. For larger values of $y/0.5b$, $\bar{u}/u_s$ gradually increases.

Determination of Shear Velocity

Because of the difficulties involved in the direct measurement of the wall shear stress, the shear velocity u_* is calcu-

lated usually by indirect methods. Keulegan (1938), Kamphuis (1974), and Blumberg et al. (1992) used the expression $u_* = \sqrt{ghS}$ or $u_* = \sqrt{gRS}$ where S is the water surface slope. Some investigators have obtained the shear velocity from an assumed velocity distribution, for instance using the law of the wall (Zippe and Graf 1983; Steffler et al. 1985; Cardoso et al. 1989) or using a power law (Sarma et al. 1983). Nezu and Rodi (1986) determined the shear velocity using the total shear stress $\tau = \mu du/dz - \rho u'w'$ where μ is the dynamic viscosity, and u', w' are the turbulent velocity fluctuations.

Kırkgöz (1989) obtained the shear velocities using the measured velocity distributions in the viscous sublayer. By assuming a linear velocity distribution in the viscous sublayer the shear velocity can be derived from the Newton's law of viscosity as

$$u_* = \sqrt{\nu \frac{u}{z}} \qquad (6)$$

where u represents the velocity in the viscous sublayer at a distance z from the smooth bed. In the present study the shear velocities are determined using (6). The measured bed velocities have the linear portion of the velocity distributions within the viscous sublayer from 0.3 to 1.0 mm in height, depending on the experimental conditions. In the experiments it was possible to measure the flow velocity as near to the smooth bed as 0.3 mm. Therefore, the linear velocity distribution in the viscous sublayer became apparent in almost all measured velocity profiles, such as in Fig. 7.

Table 2 gives the calculated shear velocities at some of the measured verticals along the channel and across the fully developed flow section. The shear velocities along the centerline of the developing zone show only small and random fluctuations. Therefore, it may be concluded that in the turbulent boundary layer of open channel flow the shear velocity remains approximately constant in the direction of flow as long
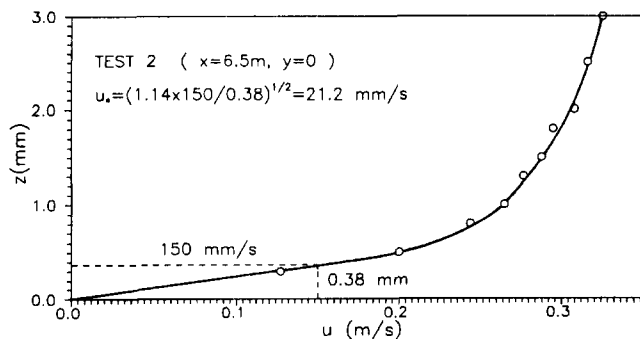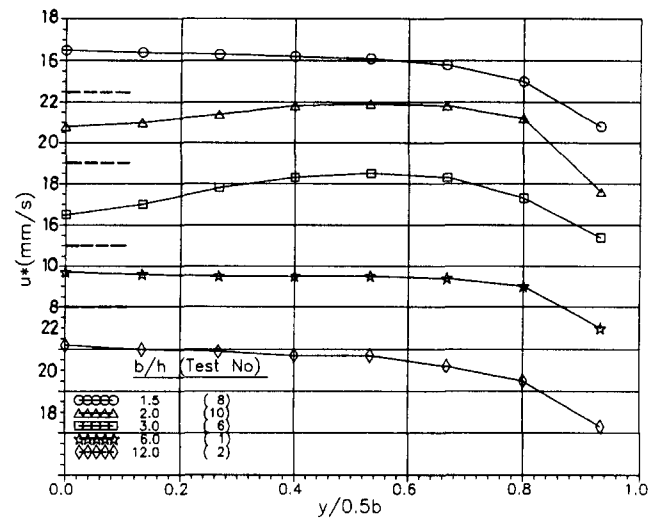

FIG. 8. Variation of Shear Velocity across Section of Fully Developed Flow of Different Aspect Ratios

as the flow conditions are not changed. On the other hand, however, Table 2 indicates variations of shear velocity across the flow section. Fig. 8 shows these variations across the fully developed flow of various aspect ratios. For aspect ratios 1.5, 6, and 12 these variations are almost similar with a steady decrease toward the sidewall. For aspect ratios 2 and 3 u_* first increases and then decreases. This oscillatory behavior of u_* has a maximum for $b/h = 3$. Similar variations of bed-shear stress across the flow section were reported by Knight and Patel (1985). It was explained by the positioning of the secondary current cells created by the corner boundaries in straight channels. Nezu et al. (1993) also stated that the bed-shear stress is influenced by the secondary flow in open channels.

Law of the Wall Distribution

Figs. 9–12 show the law of the wall distributions of the measured velocities at $x = 1.1$, 2.5, 4.0, and 5.5 m for $y = 0$. They represent the velocity profiles in the flow developing zone. However, as mentioned earlier, the length of the flow developing zone varies approximately between 1.7 and 6.5 m depending on the test conditions. Therefore Figs. 10–12 also include data of fully developed flow for some tests (see Table 1). Figs. 13, 15, and 17 give the law of the wall distributions of fully developed flow at $y = 0$, 0.06, and 0.12 m for $x = 6.5$ m based on the shear velocities in Table 2.

In all of the law of the wall distributions, the experimental data fit a linear relationship in the viscous sublayer of developing and fully developed flow. When $u_* z/\nu \leq 10$ the velocity distribution can be given by

$$\frac{u}{u_*} = \frac{u_* z}{\nu} \qquad (7)$$

the law of the wall equation [see (1)] with $\chi = 0.41$ and $B = 5.5$ takes the following form:

$$\frac{u}{u_*} = 2.44 \ln \frac{u_* z}{\nu} + 5.5 \qquad (8)$$

plotted in Figs. 9–13, 15, and 17. The agreement between (8) and the experimental data is quite satisfactory in the turbulent inner region. The average lower limit of the range of agreement changes from about $u_* z/\nu = 20$ to 40 along the measured flow length, i.e., the transition between the viscous sublayer and the turbulent inner region increases as the flow develops.
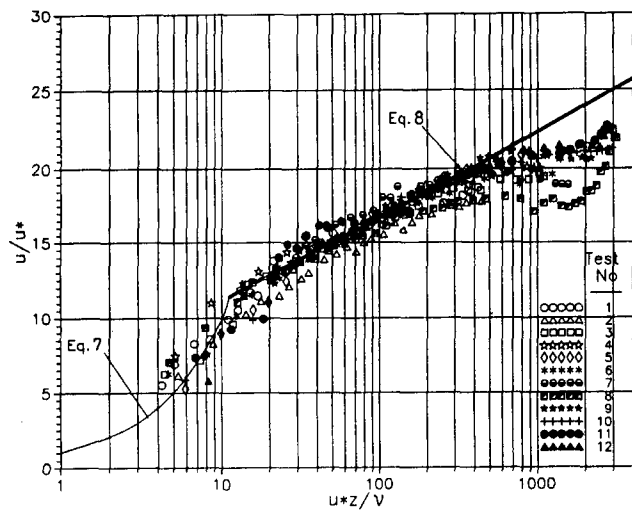

FIG. 7. Velocity Profile near Channel Bed

TABLE 2. Calculated Shear Velocities

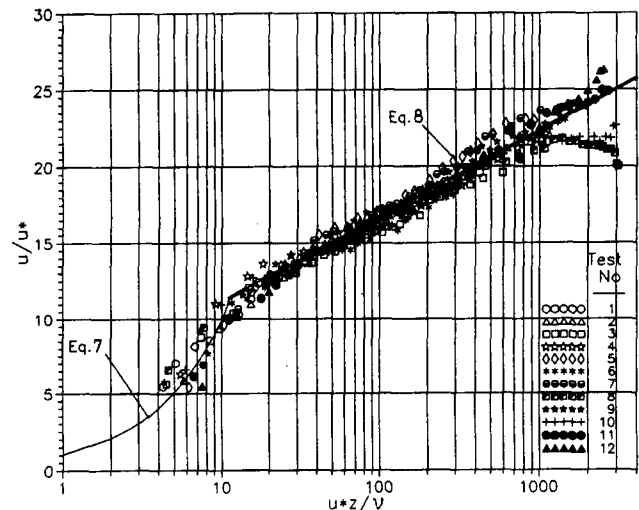| Test number (1)	Shear Velocity u_* (mm/s) at Verticals: x (m) and y (m)						
	1.1, 0 (2)	2.5, 0 (3)	4.0, 0 (4)	5.5, 0 (5)	6.5, 0 (6)	6.5, 0.06 (7)	6.5, 0.12 (8)
1	9.6	9.8	9.7	9.7	9.7	9.5	9.0
2	20.2	21.4	21.8	21.8	21.2	20.7	19.5
3	16.2	16.5	17.0	16.9	16.7	17.0	15.6
4	19.5	19.5	20.6	20.8	21.3	22.0	20.4
5	22.4	23.3	23.0	23.5	23.5	23.5	20.2
6	17.6	17.3	17.0	16.5	16.5	18.3	17.3
7	29.6	29.6	29.8	29.0	28.5	28.0	27.0
8	17.8	19.0	18.3	17.5	16.5	16.2	15.0
9	30.8	31.5	31.0	31.0	30.8	31.7	29.6
10	22.3	23.0	22.1	22.5	20.8	21.8	21.2
11	26.0	26.4	25.7	25.3	25.7	27.0	26.5
12	31.2	29.9	28.8	28.5	29.8	31.5	29.5

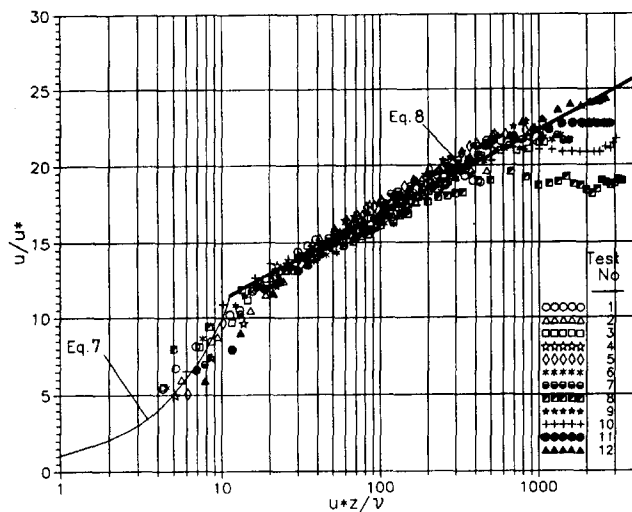**FIG. 9.** Law of the Wall Distribution at $x = 1.1$ m, $y = 0$

FIG. 10. Law of the Wall Distribution at $x = 2.5$ m, $y = 0$

FIG. 11. Law of the Wall Distribution at $x = 4.0$ m, $y = 0$

FIG. 12. Law of the Wall Distribution at $x = 5.5$ m, $y = 0$

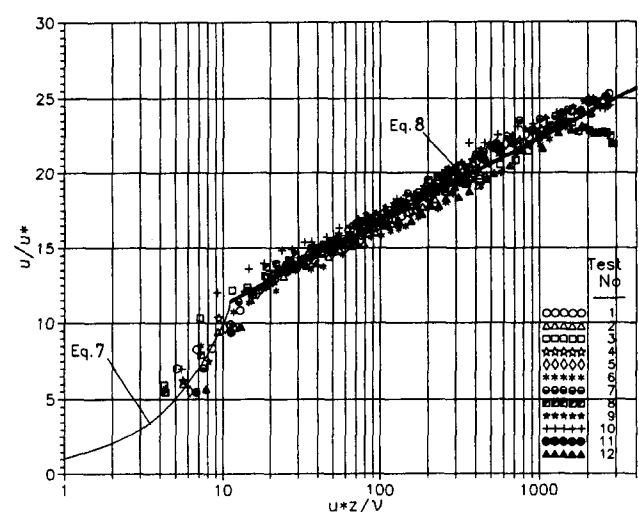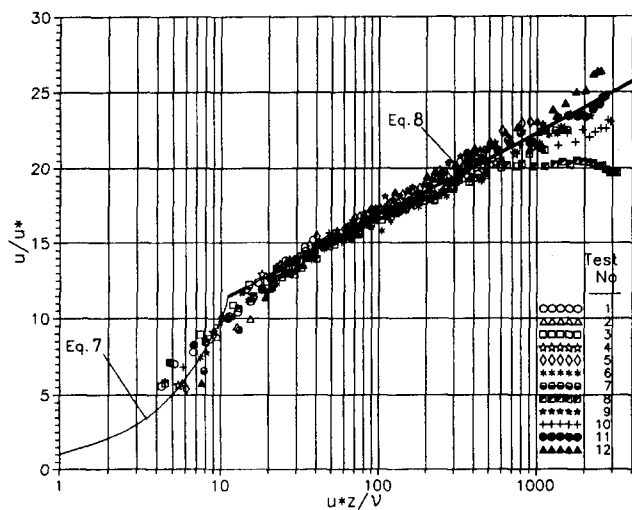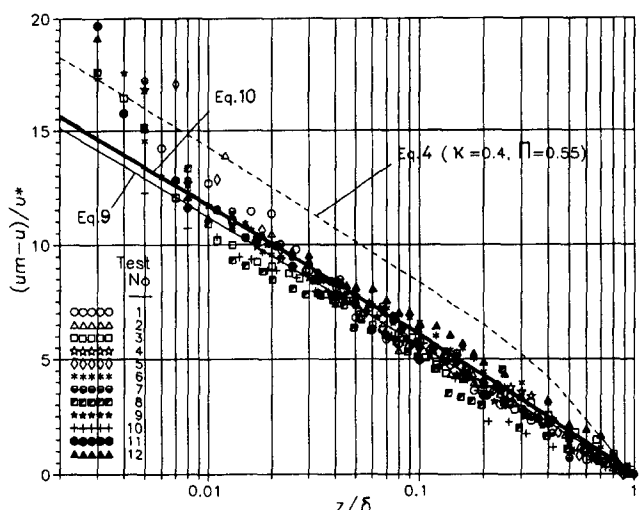**FIG. 13.** Law of the Wall Distribution at $x = 6.5$ m, $y = 0$

FIG. 14. Velocity-Defect Distribution at $x = 6.5$ m, $y = 0$

The velocity profiles in Fig. 9 are all measured in the flow developing zone and no wake effect can be detected. In the following figures, that is toward the fully developed flow section of all tests at $x = 6.5$ m, the wake effect becomes more and more apparent. The upper applicability limit of (8) depends on the flow conditions. The wake effect starts at about $u_*z/\nu = 200$ for all measured verticals. Figs. 13, 15, and 17

show that the law of the wall distributions have almost the same pattern across the fully developed flow section.

Velocity-Defect Distribution

The velocity-defect distributions of the mean velocities for three verticals of the fully developed flow at $x = 6.5$ m are
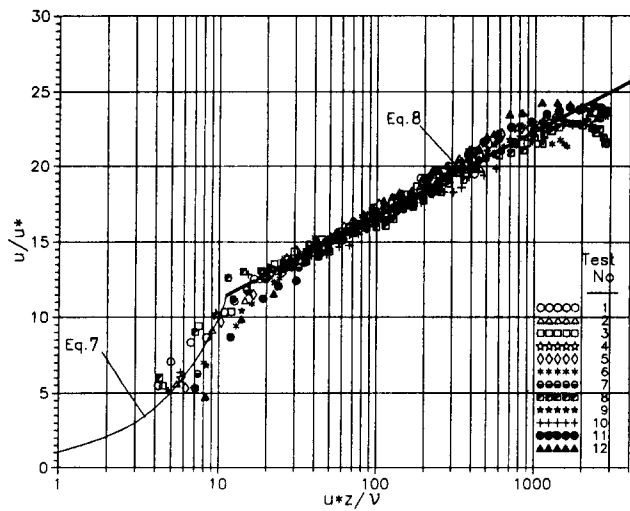
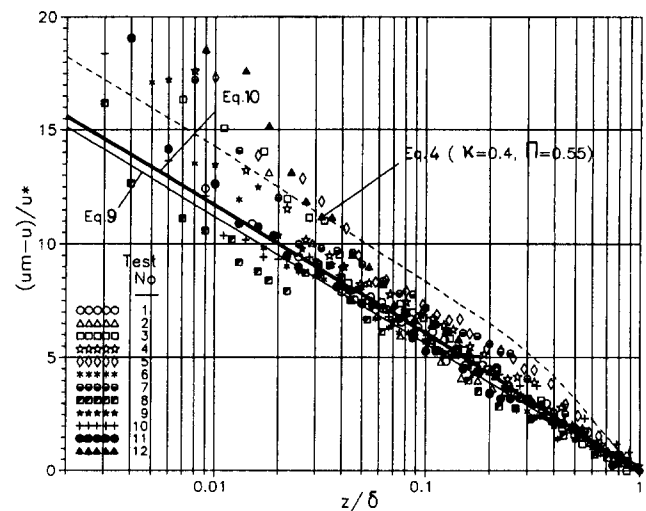**FIG. 15. Law of the Wall Distribution at *x* = 6.5 m, *y* = 0.06 m**
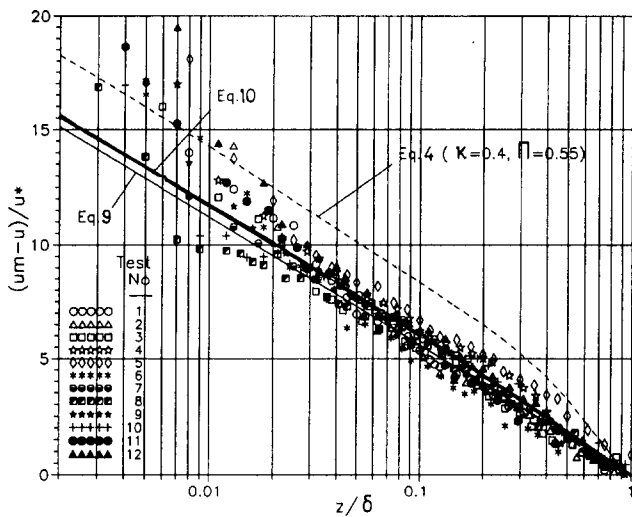
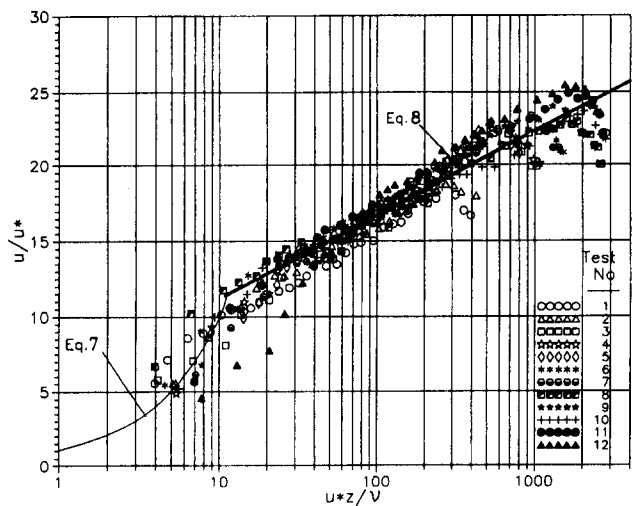**FIG. 16. Velocity-Defect Distribution at *x* = 6.5 m, *y* = 0.06 m**

FIG. 17. Law of the Wall Distribution at *x* = 6.5 m, *y* = 0.12 m

given in Figs. 14, 16, and 18. The velocity-defect formulas [see (3) and (4)] are drawn with $\chi = 0.41$ and $\Pi = 0.1$, i.e.

$$\frac{u_m - u}{u_*} = -2.44 \ln \frac{z}{\delta} \qquad (9)$$

and

FIG. 18. Velocity-Defect Distribution at *x* = 6.5 m, *y* = 0.12 m

$$\frac{u_m - u}{u_*} = -2.44 \ln \frac{z}{\delta} + 0.488 \cos^2 \left(\frac{\pi z}{2\delta}\right) \qquad (10)$$

Eq. (4), with Coles's parameters $\chi = 0.4$ and $\Pi = 0.55$ also are included in Figs. 14, 16, and 18. It may be concluded that the overall experimental data for the vertical mean velocity distribution of fully developed flow agree reasonably well with the velocity-defect formula, [see (10)] modified by Coles. However, (4), with Coles's original parameters $\chi = 0.4$ and $\Pi = 0.55$, seems to depart from the experimental data.

CONCLUSIONS

From the experimental study of velocity profiles of developing and fully developed smooth open channel flow the following conclusions may be drawn:

1. There is a linear relationship between the dimensionless length L/h of the turbulent flow developing zone of open channel flow and the ratio R/F.
2. At the axis of a fully developed turbulent flow section the boundary layer extends to the water surface if the channel aspect ratio $b/h \geq 3$.
3. For the present experimental conditions, the ratio of the average velocity and the surface velocity varies between 0.88 and 1.00 at the verticals within the 60% middle portion of the channel width.
4. For narrow and wide channel sections the shear velocity gradually decreases toward the sidewall. However, close to $b/h = 3$, the shear velocity varies in an oscillatory manner between the centerline and sidewall of the channel. Shear velocities along the flow developing zone seem to remain almost unchanged.
5. In the turbulent part of the inner region of developing and fully developed boundary layers on a smooth bed, the experimental velocity profiles agree reasonably well with the logarithmic law of the wall distribution, for coefficients $A = 2.44$ and $B = 5.5$.
6. According to the results of the present study the wake effect on the boundary layer velocity profiles is weak in the developing boundary flow. In the fully developed boundary flow the velocity-defect equation modified by Coles follows the measured velocity profiles better in the inner and outer regions if the profile parameter is taken as 0.1.

ACKNOWLEDGMENT

APPENDIX I.   REFERENCES

Ardıçlıoğlu, M. (1994). "Investigatiion of turbulent velocity profile in smooth open channel flows," PhD thesis, University of Çukurova, Adana, Turkey (in Turkish).

Bayazit, M. (1976). "Free surface flow in a channel of large relative roughness." *J. Hydr. Res.*, Delft, The Netherlands, 14(2), 115–126.

Blumberg, A. F., Galperin, B., and O'Connor, D. J. (1992). "Modeling vertical structure of open channel flows." *J. Hydr. Engrg.*, ASCE, 118(8), 1119–1134.

Cardoso, A. H., Graf, W. H., and Gust, G. (1989). "Uniform flow in a smooth open channel." *J. Hydr. Res.*, Delft, The Netherlands, 27(5), 603–616.

Cebeci, T., and Smith, A. M. O. (1974). *Analysis of turbulent boundary layers*. Academic Press, Inc., New York, N.Y.

Clauser, F. H. (1956). "The turbulent boundary layer." *Advances in Appl. Mech.*, 4, 1–51.

Coles, D. (1956). "The law of the wake in the turbulent boundary layer." *J. Fluid Mech.*, Cambridge, U.K., 1, 191–226.

Gaddini, B., and Morganti, M. (1982). "Turbulent shear-stresses and velocity distribution in open channel flows." *La Houille Blanche*, 37(4), 309–325.

Kamphuis, J. W. (1974). "Determination of sand roughness for fixed beds." *J. Hydr. Res.*, Delft, The Netherlands, 12(2), 193–203.

Keulegan, G. H. (1938). "Laws of turbulent flow in open channels." *J. Res.*, Nat. Bureau of Standards, Washington, D.C., 21, 707–741.

Kırkgöz, M. S. (1989). "Turbulent velocity profiles for smooth and rough open channel flow." *J. Hydr. Engrg.*, ASCE, 115(11), 1543–1561.

Klebanoff, P. S. (1954). "Characteristics of turbulence in a boundary layer with zero pressure gradient." *NACA Tech. Notes No. 3178*, Washington, D.C.

Knight, D. W., and Patel, H. S. (1985). "Boundary shear in smooth rectangular ducts." *J. Hydr. Engrg.*, ASCE, 111(1), 29–47.

Maclean, A. G. (1991). "Open channel velocity profiles over a zone of rapid infiltration." *J. Hydr. Res.*, Delft, The Netherlands, 29(1), 15–27.

Nezu, I., and Rodi, W. (1986). "Open channel flow measurements with a Laser Doppler Anemometer." *J. Hydr. Engrg.*, ASCE, 112(5), 335–355.

Nezu, I., Tominaga, A., and Nakagawa, H. (1993). "Field measurements of secondary currents in straight rivers." *J. Hydr. Engrg.*, ASCE, 119(5), 598–614.

Nikuradse, J. (1932). "Gesetzmässigkeiten der turbulenten Strömung in glatten Rohren." *Forsch. Geb. Ing.-Wes.*, Heft 356, Berlin (in German).

Prandtl, L. (1925). "Über die ausgebildete Turbulenz." *Z. Angew. Math. Mech.*, 5, 136–139 (in German).

Prandtl, L. (1932). "Zur turbulenten Strömung in Rohren und längs Platten." *Ergebnisse der Aerodynamischen Versuchsanstalt zu Göttingen*, 4, 18–29 (in German).

Sarma, K. V. N., Lakshminarayana, P., and Rao, N. S. L. (1983). "Velocity distribution in smooth rectangular open channels." *J. Hydr. Engrg.*, ASCE, 109(2), 270–289.

Schlichting, H. (1968). *Boundary layer theory*. McGraw-Hill, Inc., New York, N.Y.

Steffler, P. M., Rajaratnam, N., and Peterson, A. W. (1985). "LDA measurements in open channel." *J. Hydr. Engrg.*, ASCE, 111(1), 119–130.

Townsend, A. A. (1956). *The structure of turbulent shear flow*. Cambridge University Press, New York, N.Y.

Tominaga, A., and Nezu, I. (1992). "Velocity profiles in steep open channel flows." *J. Hydr. Engrg.*, ASCE, 118(1), 72–90.

von Kármán, T. (1930). "Mechanische Ähnlichkeit und Turbulenz." *Göttinger Nachrichten, Math. Phys. Klasse*, 58–60 (in German).

Zippe, H. J., and Graf, W. H. (1983). "Turbulent boundary-layer flow over permeable and non-permeable rough surfaces." *J. Hydr. Res.*, Delft, The Netherlands, 21(1), 51–65.

APPENDIX II.   NOTATION

The following symbols are used in this paper:

b = width of channel;
F = Froude number;
g = gravitational acceleration;
h = depth of flow;
L = length of flow developing zone;
Q = rate of flow;
R = hydraulic radius;
R = Reynolds number;
u = mean flow velocity;
$\bar{u}$ = averge velocity for unit width;
u_m = maximum mean velocity in the distribution;
u_s = surface velocity;
u_* = shear velocity;
V = average flow velocity;
x = distance from the channel entrance;
y = transverse horizontal distance from the centerline of channel bed;
z = vertical distance from channel bed;
δ = thickness of boundary layer;
χ = von Kármán constant;
ν = kinematic viscosity;
Π = profile parameter;
ρ = density; and
τ_0 = bed-shear stress.